Proceedings of 20th International Congress on Acoustics, ICA 2010

23-27 August 2010, Sydney, Australia

# Aspects of practical models of acoustic reflection loss at the ocean surface

**Adrian D. Jones (1), Alec J. Duncan (2), Amos Maggi (2), Paul A. Clarke (1) and Janice Sendt (3)**

(1) Defence Science and Technology Organisation, P.O. Box 1500, Edinburgh, SA 5111, Australia
(2) Centre for Marine Science & Technology, Curtin University of Technology, GPO Box U1987, Perth WA 6845, Australia
(3) Thales Australia, 274 Victoria Road, Rydalmere, NSW 2116, Australia

**PACS: 43.30.-K, 43.30.HW, 43.20.FN**

## ABSTRACT

Modelling the reflection of acoustic signals at a realistic ocean surface, particularly at small angles of incidence, is an area of underwater acoustics for which no known solution exists. For mid-frequencies and above (over about 1 kHz), there exist a number of complex phenomena, each of which imposes considerable complexity. These include: the two-dimensional sea surface shape formed from local wind and distant swell; acoustic shadowing of parts of the surface to sound incident at small angles; diffraction of sound into the shadow zones; bubble formation from white-caps. Models used to describe sound transmission to ranges of tens of kilometres must incorporate practical sub-models of surface loss to describe the reduction in received signal due to scattering at non-specular angles. The literature of the last several decades includes many descriptions of mathematically-based studies of surface loss phenomena, however very little of this work has resulted in models for routine use. This paper reviews the situation and shows comparisons between surface loss values obtained from practical sub-models employed by the authors with, firstly, the small-slope model made available by the University of Washington and, secondly, surface loss values inferred from use of a transmission model which includes a deterministic description of the rough sea surface. In this work, particular attention has been paid to the degree of modelling complexity which is required to capture the loss phenomena evidenced by the deterministic modelling. In this extension of an earlier study by the authors, an attempt is made to include the effects of bubbles appropriate to the sea state, via adjustment of the sound speed in the bubbly region.

## INTRODUCTION

In modelling underwater acoustic phenomena, in particular, sound received at medium and long range from a source, it becomes necessary to describe the reflection of sound incident upon the ocean surface boundary. For predictions of signals received at medium-to-long ranges (10 km to 30 km or more), especially for oceans with an isothermal surface duct or for shallow oceans, the acoustic interaction at small angles of incidence (about 10° and less) is particularly relevant. Due to the roughness of the surface shape, and the effects of bubbles in the water column, some of the sound incident on the surface is scattered at non-specular angles, with this being perceived as a reflection loss. As is well known, at-sea experience has shown that these effects are significant at frequencies over about 1 kHz, but of limited relevance at lower frequencies, unless the transmission range is quite large (100 km or more).

The literature on surface loss is vast, as is well known, and extends back to the 1950s. Most of this work (e.g. [1-5]) was focussed on descriptions of loss due to the roughness of the surface. Based on the work of Marsh et al. [1], [2], and that of Beckmann and Spizzichino [6], plus with adjustments to match at-sea data (see [2]), the "Beckmann-Spizzichino" surface loss model was created (see [7, 8]). Subsequently, Kuo [4] identified errors in the analysis of Marsh et al. [1] which amounted to the loss predictions of the latter being about thee times too large in magnitude for a surface loss caused by roughness only. Kuo [4] did confirm, however, that the loss values, in dB, did adhere to a linear function of grazing angle for small angles, this feature being in the model of Marsh et al. [1]. This result implied that the RAYMODE Beckmann-Spizzichino model [7, 8] could not be regarded as a good match to the losses from roughness. Recent work carried out by Jones et al. [9-11] examined aspects of the origins of this model and showed that it is not based on rigorous application of physics, but contains features derived empirically. It must be noted, however, that that work by Jones et al. showed that the incorporation of either of two implementations of the Beckmann-Spizzichino model into Transmission Loss (*TL*) calculations gave reasonable agreement with at-sea data for some scenarios when two models based solely on roughness effects under-estimated the measured loss.

The failure of roughness-only models to describe at-sea transmission data is known anecdotally, but direct comparisons are seldom seen in the literature. Recently, Ainslie [12] showed that if the refractive effects caused by wind-generated bubbles were included in a modelling of *TL* which also incorporated the surface losses described by roughness alone, the resultant outcome gave a good match to at-sea data in the frequency range 1 – 4 kHz. The authors of the present

paper chose to extend the work of an earlier study [11] by including the refractive effects of bubbles, and due to the reported success of Ainslie, have chosen to adopt the same model of bubble refraction.

This paper commences with a review of the surface loss models under investigation, where it may be noted that all those considered were assumed to be based on the physics describing the scattering loss from a roughened sea surface for a bubble-free ocean. Particular attention is given to the Kirchhoff model and its relativity to the small-slope model of Williams et al. [5]. (The authors acknowledge that the latter model was made available for this purpose by the Applied Physics Laboratory of the University of Washington, Seattle.) In particular, the Kirchhoff model is expected to fail at small grazing angles if the radius of the sea surface is less than a certain value. Next, descriptions are given of the deterministic, numerical technique used by the authors from the Centre for Marine Science & Technology (CMST) at the Curtin University of Technology for the determination of surface loss per bounce. Values of loss so determined are compared with loss values returned by the Kirchhoff and Williams et al. surface loss models. Lastly, the techniques for modifying the sound speed profile (SSP) to include the effects of bubbles are reviewed, and the *TL* values obtained with a combination of the Williams et al. small-slope roughness model and the modified SSP are shown with reference to bubble-free data. To maintain comparison with the work of Williams et al., the acoustic frequency selected for study is 3200 Hz and wind speeds are 5 m/s and 10 m/s.

## SURFACE LOSS MODELS STUDIED

The surface loss models considered include the Kirchhoff, two implementations of Beckmann-Spizzichino and the small-slope model from the Applied Physics Laboratory of the University of Washington, Seattle [5].

### Kirchhoff

The Kirchhoff, or tangent plane, approximation [13] is based on the assumption that the reflection at any, and every, location on the surface occurs as if the surface was locally flat. As stated by Ogilvy [13] section 6, for example, the requirement for flatness implies that the radius of curvature of the surface $\rho$, in metres, must be sufficiently large that $k\rho\sin^3\beta >> 1$, where $\beta$ is the grazing angle with the mean surface plane, radians; $k$ is acoustic wavenumber $2\pi f/c_w$; $f$ is cyclic frequency, Hz; $c_w$ is speed of sound in seawater, m/s. Evaluation for expected values of $\rho$ (guessed to be in the range 20 m to 100 m) shows that this will be satisfied for 3.2 kHz at grazing angles exceeding about 9° to 5°, respectively, but not for grazing angles of the order 2° to 3° typical of surface ducts. A further assumption usually applied to closed-form evaluations of surface loss is that a direction normal to the surface is assumed approximately the same as a normal to the mean plane (e.g. Ogilvy [13] section 6.2). This will be accurate for small slopes.

For the Kirchhoff surface loss model, the sole input describing the surface is the rms wave height $h_\sigma$. As stated by Williams et al. [5] (section V), it is immaterial as to whether $h_\sigma$ is obtained using a surface description in either one, or two, surface dimensions. The standard form of the Kirchhoff loss model for a surface with a Gaussian distribution of heights is well known, e.g. see Lurton [14] section A.3.3. Here, the surface loss in dB is commonly expressed in terms of the Rayleigh roughness parameter $\Gamma = \left(4\pi f h_\sigma \sin\beta\right)/c_w$. The result does not depend on a spatial correlation with range (e.g. Brekhovskikh and Lysanov [15]). The loss mechanism is the phase cancellation of the phase separated components of an incident plane wave, reflected from the entire insonified area, thus representing a coherent loss component.

In an earlier paper [11] the authors mentioned that a Kirchhoff model may be obtained for non-Gaussian distributions of surface heights. Expressions were presented for Kirchhoff loss models derived for each of a symmetrical triangular-shaped, and a sinusoidal-shaped surface [11], using a surface description in one-dimension. An interesting conclusion was that, if rms roughness was made the same for each type of surface height distribution, the values of surface loss were nearly the same for grazing angles less than about 10°. This suggests that the rms roughness, not the distribution of surface heights, is the important factor.

Apart from the limitations mentioned earlier, the Kirchhoff model may be expected to fail when the wave slope exceeds the slope of an incoming plane wave. In such circumstances, there will be a shadowing effect (e.g. see Wagner [16]), and the complication of diffraction of sound into the shadow zones. Nonetheless, the Kirchhoff model is appealing, as it has only a single parameter.

### Small Slope Model of Williams et al.

Williams et al. [5] published details of a small-slope approximation model, and a perturbation analysis model. These models have been made available to the lead author for the purposes of this work. Each model describes the coherent surface reflection coefficient due to surface roughness with a Pierson-Moskowitz surface wave spectrum.

### Beckmann-Spizzichino

Each of DSTO and Thales Australia retains implementations of the "Beckmann-Spizzichino" model of surface loss. This model has a long history of use and its origins are in the 1960s (e.g. Jones et al. [9-11]). The RAYMODE Beckmann-Spizzichino model is described in two NORDA documents (Lauer [7], McGirr [8]), with some of the links to the underlying theory being clarified by Jones et al. [9-11], wherein the algorithms of the RAYMODE version are outlined.

### Comparison of surface loss models

In an earlier paper by the authors [11] figures of surface loss values were generated for the models discussed above, for a single surface bounce for a frequency of 3200 Hz. These figures are reproduced below, and an extra figure is included, as they are referenced later in the text. Figs. 1, 2 and 3 show these data, as a function of grazing angle, for wind speeds of 5 m/s, 7.5 m/s and 10 m/s. The rms surface height $h_\sigma$ for the Kirchhoff model was obtained using the following expression, which is derived from the Pierson-Moskowitz wave spectrum (e.g. section 13.1 of Medwin and Clay [17]):

$$h_\sigma \approx 5.3\times10^{-3} w^2 , \quad (1)$$

where wind speed $w$ is in m/s. (Note: $w$ is usually taken to be at 19.5 m above sea level.) For wind speeds used in this study, values of $h_\sigma$ are 0.13 m (5 m/s wind speed), 0.30 m (7.5 m/s wind speed) and 0.53 m (10 m/s wind speed).

For small grazing angles, the Kirchhoff model gives a dependence on the square of grazing angle [11]. This is apparent in each figure. From these figures it is apparent that the Williams et al. small slope model gives a linear dependence on grazing angle for small angles, but becomes closer to the Kirchhoff result at about 7° for 5 m/s wind speed, 5° for

7.5 m/s wind speed and 3° for 10 m/s wind speed. As mentioned earlier, it may be expected that for grazing angles less than some limiting value, the Kirchhoff model may be expected to fail due to the radius of curvature of the ocean surface. It becomes appealing to establish a rationale for estimating this limiting grazing angle, according to the prevailing circumstances, so that the simple Kirchhoff result might be merged with an expected linear function in grazing angle for smaller angles and a result similar to the Williams et al. small slope model might be achieved. An incentive for this is that the Kirchhoff model might then be rapidly altered to suit observable surface profiles that do not necessarily adhere to a particular surface wave spectrum.

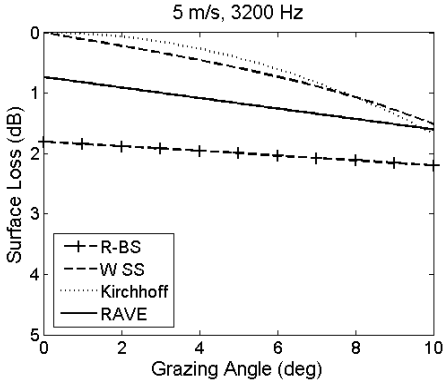


**Figure 1**. Surface Loss per bounce 5 m/s wind speed, 3200 Hz

where:

| | |
|---|---|
| R-BS | RAYMODE Beckmann-Spizzichino |
| W SS | Williams et al. small slope model |
| Kirchhoff | Gaussian roughness Kirchhoff model (2) |
| RAVE | Beckmann-Spizzichino of Thales Australia |

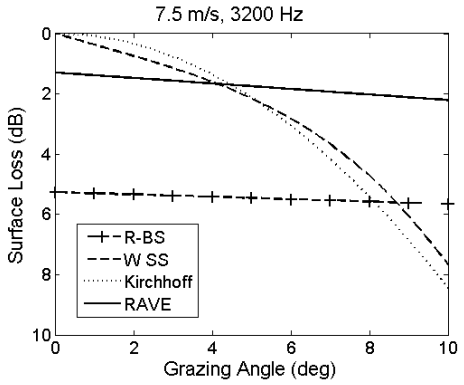


**Figure 2**. Surface Loss per bounce for 7.5 m/s wind speed, 3200 Hz

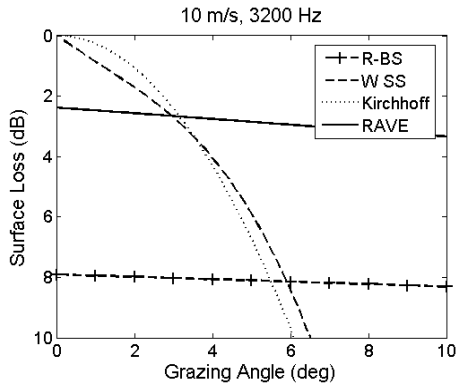


**Figure 3**. Surface Loss per bounce for 10 m/s wind speed, 3200 Hz

The Beckmann-Spizzichino models are quite different from the others, in that they do not trend to zero loss for zero grazing angle, and the loss values do not change greatly with grazing angle. The RAVE implementation of Beckmann-Spizzichino has a similar lack of variation with grazing angle as does the RAYMODE version, but has lower loss values. None of these four models implicitly includes the effects of shadowing of the surface, but such effects might be expected to increase the loss for small grazing angles and rough surfaces. The Beckmann-Spizzichino data in Figs. 1, 2 and 3 may be considered to represent this effect (finite loss at grazing angle 0.0°).

## DETERMINISTIC MODELLING OF SURFACE LOSS

Values of coherent surface reflection loss were determined by the CMST at Curtin University through a numerical simulation of transmission in an ocean with a sea surface boundary displaced vertically according the Pierson-Moskowitz wave spectrum. By using a PE transmission code (RAMSurf [18] as implemented by the CMST [19]) the modelling included forward transmission effects due to acoustic shadowing of segments of the sea surface and diffraction of sound into shadowed zones. The initial results from this work were described in an earlier paper [11], however, a more complete description of the technique, and of the results to date, are included below.

For practical purposes, a one-dimensional sea surface was described and transmission was simulated for cylindrical symmetry. The scenarios were devised so that, for each, transmission to ranges of interest occurred after interaction at the surface at known small angles of incidence.

### Technique for Determination of Coherent Surface Loss Values

In practice, the CMST simulation generated sea surface height values with a spatial correlation, with range, determined by the Pierson-Moskowitz wave spectrum, and a surface height distribution which was Gaussian, with rms wave height $h_\sigma$ related to wind speed according to (1). The range interval at which the surface height was sampled was 3 m. (This interval was selected as the RAMSurf model was limited to 10,000 range points, and a maximum range of 30 km was desired.). The grid sizes used for the PE modelling of the acoustic field were 0.1λ vertically, and 2λ horizontally, where λ is acoustic wavelength. The acoustic field was computed to a range of 30 km in each case. For each scenario, the field was computed, first using a description of a flat, perfectly reflective surface, then with the surface described as rough, as above. For each scenario, a large number (typically 40) of replications of the sea surface was generated and the coherent field determined for each. The total loss of coherent transmission was determined by subtracting the mean of the coherent pressure fields obtained for the roughened surface from the field obtained with the smooth surface.

In order to determine a coherent surface reflection loss per surface bounce, scenarios were selected so that each consisted of a surface duct of uniform gradient over an isovelocity ocean layer of 110.3 m thickness, under which was placed an absorbing lower boundary. The (omni-directional) source was placed 5 m above the lower boundary of the surface duct. This ensured that all surface reflections occurred at grazing angles that were very close to those expected for the limiting ray for the surface duct. By this technique, grazing angles were thus pre-selected. Subsequent ray modelling was used to determine the small spread of rays applicable for transmission for each scenario, so that a finer resolution of the aver-

aged surface grazing angle associated with each scenario might be determined. Combinations of duct depth and gradient were selected to ensure that the modelled frequency was well above that required for duct trapping, to minimise duct leakage. Surface loss per bounce was determined by dividing total coherent loss in dB, as determined within the duct, by the number of surface skips. Fig. 4 shows an example of this work for wind speed 5 m/s and source frequency 3200 Hz, for a 150 m surface duct of gradient 0.20 $s^{-1}$, for which the following may be obtained from ray theory: grazing angle for limiting ray 11.5°, duct trapping frequency 28 Hz, skip distance 3 km. Fig. 4 shows values of coherent loss as a function of range at (i) duct mid-depth and (ii) receiver depth equal to source depth. A similar loss per bounce is evident at each depth, as are each of the surface bounces. The coherent surface loss per bounce at 11.5° follows as 1.4 dB.

Whilst it was possible to achieve multiple surface bounces for most of the grazing angles modelled, the smaller grazing angles presented the greatest modelling challenges. For the scenario with the smallest grazing angle modelled, 1.15°, a small sound speed gradient $g$ = 0.005 $s^{-1}$ was used with a duct depth 60 m. If the duct is deeper, the grazing angle is increased, but if the duct is shallower, the cut-off frequency for the duct becomes too high for highly multi-modal transmission to occur for the modelled frequency 3200 Hz. An increase in gradient increases the grazing angle, whereas a decrease in gradient results in a surface skip distance in excess of the 30 km maximum range available for this study.

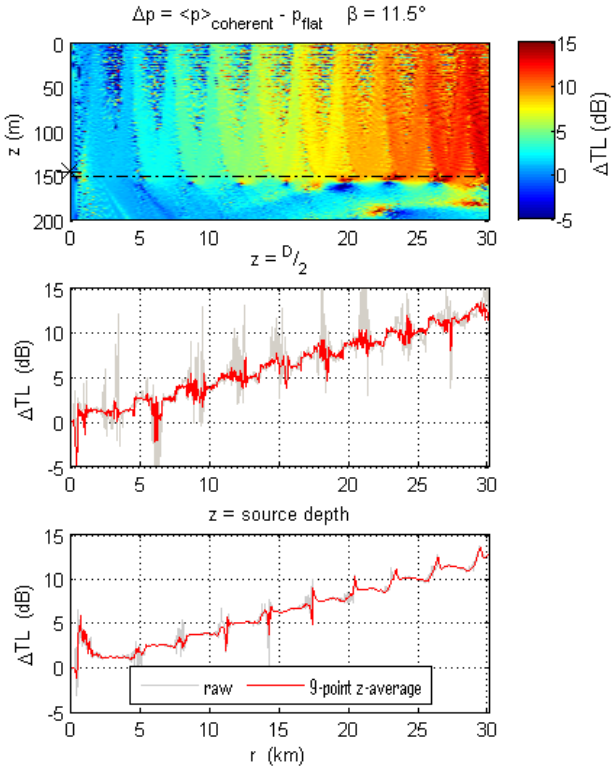


**Figure 4**. Overall coherent loss for ducted transmission, surface skips at 11.5° grazing angle, 5 m/s wind speed, 3200 Hz

The scenarios used in this study, and their nominal surface grazing angles are shown in Table 1. It is to be noted that source depth was 5 m less than the duct depth in each case. The values of grazing angle for the limiting ray β, surface skip distance $r_s$, and duct cut-off frequency $f_{sd}$, are also shown. These were derived from the standard surface duct relationships (e.g. Etter [20] section 5.2.1).

**Table 1**. Surface duct scenarios modelled at 3200 Hz

| Duct depth $D$ | Sound speed gradient $g$ | skip distance $r_s$ | surface grazing angle β | Duct cut-off frequency $f_{sd}$ |
|---|---|---|---|---|
| 60 m | 0.005 $s^{-1}$ | 12.0 km | 1.15° | 700 Hz |
| 100 m | 0.005 $s^{-1}$ | 15.5 km | 1.5° | 330 Hz |
| 70 m | 0.01 $s^{-1}$ | 9.2 km | 1.75° | 390 Hz |
| 100 m | 0.01 $s^{-1}$ | 10.9 km | 2.1° | 230 Hz |
| 60 m | 0.017 $s^{-1}$ | 6.5 km | 2.1° | 430 Hz |
| 100 m | 0.017 $s^{-1}$ | 8.4 km | 2.7° | 200 Hz |
| 30 m | 0.02 $s^{-1}$ | 4.2 km | 1.6° | 990 Hz |
| 45 m | 0.02 $s^{-1}$ | 5.2 km | 2.0° | 540 Hz |
| 60 m | 0.02 $s^{-1}$ | 6.0 km | 2.3° | 351 Hz |
| 100 m | 0.02 $s^{-1}$ | 7.7 km | 3.0° | 163 Hz |
| 45 m | 0.05 $s^{-1}$ | 3.3 km | 3.1° | 340 Hz |
| 60 m | 0.05 $s^{-1}$ | 3.8 km | 3.6° | 220 Hz |
| 100 m | 0.05 $s^{-1}$ | 4.9 km | 4.7° | 100 Hz |
| 150 m | 0.05 $s^{-1}$ | 6.0 km | 5.7° | 55 Hz |
| 30 m | 0.20 $s^{-1}$ | 1.34 km | 5.1° | 310 Hz |
| 45 m | 0.20 $s^{-1}$ | 1.6 km | 6.3° | 170 Hz |
| 60 m | 0.20 $s^{-1}$ | 1.9 km | 7.2° | 110 Hz |
| 100 m | 0.20 $s^{-1}$ | 2.4 km | 9.4° | 50 Hz |
| 150 m | 0.20 $s^{-1}$ | 3.0 km | 11.5° | 28 Hz |

Source: (Authors, 2010)

## Simulation Results and Discussion

Values of coherent surface reflection loss determined by this process are shown in Figs. 5 and 6 for wind speeds 5 m/s and 10 m/s. These numerically-derived data are shown by rectangles which relate to the scatter in the data. The height of each rectangle represents the spread ±2 standard errors of the mean loss value, whereas the width represents the span of angles over which the trapped beam of rays from the source impinges on the ocean surface.

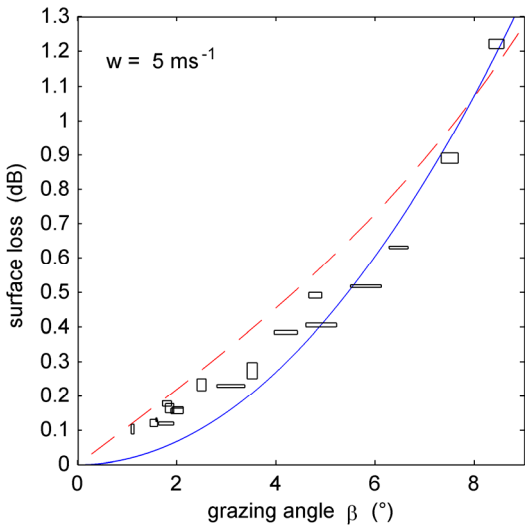


**Figure 5**. Surface Loss per bounce: blue - Gaussian Kirchhoff, red dashed line - Williams et al. small slope, deterministic; 5 m/s wind speed, 3200 Hz

These values are shown compared with those from the Gaussian roughness Kirchhoff model, and from the Williams et al. small slope model. It is apparent that the deterministic modelling is supportive of the Williams et al. small slope model for the smaller angles, with all three sets of data being similar for the larger angles shown. There is little evidence of effects due to surface shadowing, for which surface loss values in excess of the Williams et al. small slope model were expected. For the deterministic modelling, the distribution of surface slopes was Gaussian with rms surface slope values

2.3° (5 m/s wind speed) and 6.3° (10 m/s wind speed). Whilst the small rms slope for the lower wind speed is not likely to result in significant shadowing, such effects might be expected with the 10 m/s wind speed, yet none was evident across the range of grazing angles smaller than the rms slope.

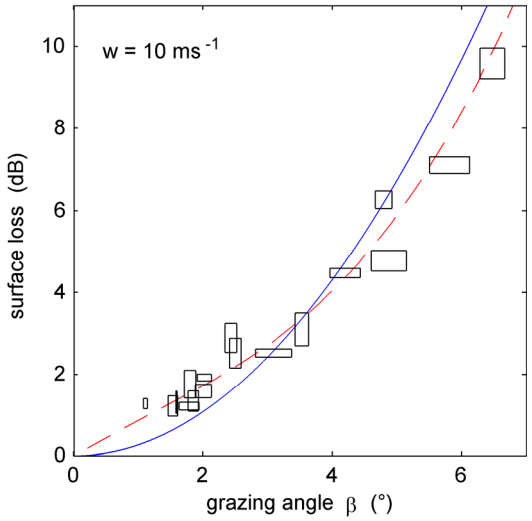


**Figure 6**. Surface Loss per bounce: blue - Gaussian Kirchhoff, red dashed line - Williams et al. small slope, deterministic; 10 m/s wind speed, 3200 Hz

### Expectations from surface radius effects

To some degree, the expectation of a non-adherence to the Kirchhoff model at small grazing angles may be anticipated from theoretical considerations, as mentioned earlier in this paper. In particular, the requirement for the validity of the Kirchhoff model may be expressed in terms of grazing angle β as

$$\sin\beta >> \left[\frac{c_w}{2\pi f \rho}\right]^{1/3} . \qquad (2)$$

It is anticipated that the failure of the Kirchhoff model, at grazing angle β given by (2), denotes the angle below which the true loss function deviates from the Kirchhoff's dependence upon the square of grazing angle. In particular, it is expected that an accurate loss function (e.g. the Williams et al. small slope model) will have a linear dependence on grazing angle, for β less than that from (2).

The CMST sea surface height values, based on numerical simulation from the Pierson-Moskowitz wave spectrum, were processed to provide distributions of the surface radius values. Here the surface radius ρ was determined as the inverse of curvature κ (e.g. see Thomas [21], section 12-6), viz.:

$$\rho = \frac{1}{\kappa} = \frac{\left[1+(dy/dx)^2\right]^{3/2}}{\pm\left(d^2y/dx^2\right)} \approx \frac{\pm 1}{\left(d^2y/dx^2\right)}, \qquad (3)$$

where it may be seen that, for small slopes $dy/dx$, the surface radius is the inverse of the second derivative of surface displacement with radial distance.

Values of radius were determined from the CMST sea surface height values sampled at the 3 m interval for each wind speed. The probability density functions $N_{|\rho|}$ of surface height obtained by this process are shown in Fig. 7.

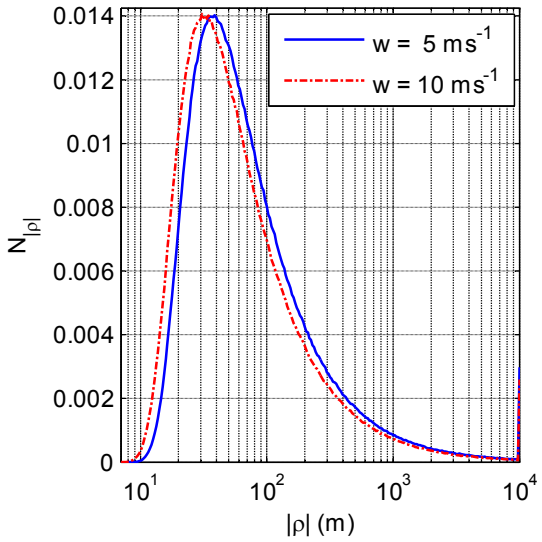


**Figure 7**. Probability density of surface radius, deterministic modelling with 5 m/s wind speed, 10 m/s wind speed, range sampling interval 3 m

The data in Fig. 7 show that the surface radius values have a large spread, but little difference is seen between the distributions at the two wind speeds. For the purpose of estimating the point of failure of the Kirchhoff model for the deterministic simulations carried out in this study, the values of ρ taken from Fig. 7 were the most likely values of surface radius for each wind speed. These values are about 40 m for 5 m/s wind speed, and 30 m for 10 m/s wind speed.

Taking the most likely value of 40 m radius for 5 m/s wind speed as corresponding with the limit for the Kirchhoff model, from (2) we get a grazing angle β of 7.0° at which the Kirchhoff model may be expected to fail. For the 10 m/s wind speed data we get a value of limiting grazing angle of 7.8°. By comparison with the data in Figs. 1 and 3, and Figs. 5 and 6, and in particular the grazing angle for which the Williams et al. loss values change from the linear form to become similar to the loss from the Kirchhoff model, these values (7.0° and 7.8°) are not identical with the data in the figures, but neither are they greatly different. The trend of these limiting angles determined from the radius data is, however, for an increase to the limiting angle with increasing wind speed, whereas the data in Figs. 1 and 3, and Figs. 5 and 6, show a contrary trend. The reason for this is not known.

It must be mentioned that the 3 metre range interval used for sampling the surface height is expected to have an impact on the derived radius values shown in Fig. 7. It is also possible that the range interval which was selected for sampling the Pierson-Moskowitz sea surface shape (also 3 metres) for input to the PE simulations of the acoustic field may have had an impact on the data shown in Figs. 5 and 6. This area is under consideration by the authors but will not be discussed further in this paper.

## INCLUSION OF BUBBLE EFFECTS

In a recent paper, Ainslie [12] outlined a technique by which he included the refractive effects of near surface bubbles, plus the absorptive effects due to the scattering caused by the bubbles. Of these effects, the refraction was the most significant, so it has been modelled in this study. As discussed below, the effect of the refraction from near-surface bubbles is to increase, significantly, the grazing angle of sound at the sea surface, so that resultant reflection loss is increased, rela-

tive to a bubble-free ocean, by virtue of the increased loss that occurs at such increased angles of incidence.

### Modifications to Sound Speed Profile

For brevity, the analysis of Ainslie [12] is not repeated here, apart from the final expression by which the sound speed values for a bubble-free ocean are modified. This is:

$$\left[\frac{c_w(z)}{c_m(z)}\right]^2 = 1 + \frac{\rho_w [c_w(z)]^2}{\kappa_0(z) P(z)} U(z) \qquad (4)$$

where $c_w(z)$, in m/s, is the speed of sound in bubble-free water as a function of depth $z$; $c_m(z)$, in m/s, is the speed of sound in bubbly water at depth $z$; $\rho_w$ is the density of bubble-free seawater in kg/m$^3$; $\kappa_0(z)$ is the polytropic index for the gas in bubbles at depth $z$ (where $\kappa_0(z) = 1.0$ for isothermal compression and $\kappa_0(z) = 1.4$ for adiabatic compression – we assumed isothermal compression herein); $P(z)$ is the absolute hydrostatic pressure, in Pa, at depth $z$; and $U(z)$ is the air fraction of seawater at depth $z$. The absolute hydrostatic pressure includes the pressure of the atmosphere plus the hydrostatic pressure to depth $z$.

The analysis of Ainslie [12] provides a means of evaluating the necessary terms in (4), and by this means a modified profile of sound speed values $c_m(z)$ is determined.

### Modelled Scenario

To demonstrate the effects of refraction caused by near-surface bubbles, a surface ducted scenario was modelled - an isothermal surface duct over an infinitely deep, isovelocity ocean:

| | |
|---|---|
| Surface duct depth $D$ | 64 m |
| Speed of sound at ocean surface | 1500 m |
| Sound speed gradient $g$ in duct | 0.017 s$^{-1}$ |
| Source, receiver depth | 18 m |
| Transmission frequency | 3200 Hz |
| Range | 30 km |

This scenario has surface duct features similar to a shallow water scenario (Track Q) for which DSTO has acoustic transmission data [11], although for the present case the effects of seafloor interaction were removed to highlight the surface loss effects. The SSP for the bubble-free water, and the SSP modified using (4) to account for near surface bubbles are shown in Fig. 8.

The top sub-figure in Fig. 8 shows the detail of the top 5 m of the SSP. In this case, the data values have been determined with a depth resolution of 0.5 m within the top 1 m, then at lesser resolution at greater depth. Clearly, the modifications to the SSP are limited to the top few metres of the ocean.

A ray plot for this scenario is shown in Fig. 9. This shows 13 rays evenly distributed in launch angle over ±1.8°, and shows the spread of angles retained with the duct. The colour coding is simply for the purpose of tracking the various ray paths, and has no other function. Although this ray plot has been obtained for the bubble-free water SSP, ray plots carried out for each of the with-bubble SSPs shown in Fig. 8 showed only miniscule deviations from the ray paths shown in Fig. 9. This presumably is due to the small extent of the water column occupied by the bubbly region.

The effect of the bubbles on the SSP is to refract the sound upward, with the effect that the angles of incidence at the surface become greater. For the source at 18 m depth, the range of possible incidence angles at the surface, as determined by a ray transmission model, are as shown in Table 2. The spread of possible launch angles for rays retained in the duct is ±1.8°.

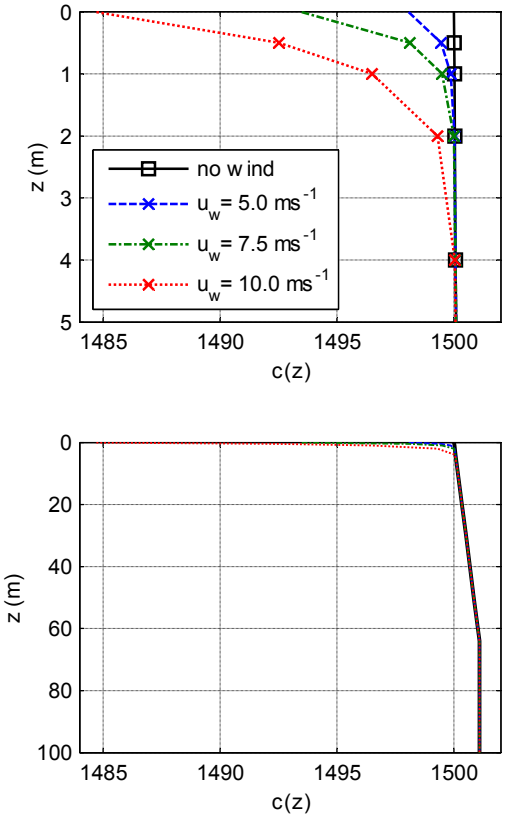


**Figure 8**. Sound speed versus depth for bubble-free water, bubbly water, wind speeds 5 m/s, 7.5 m/s, 10 m/s

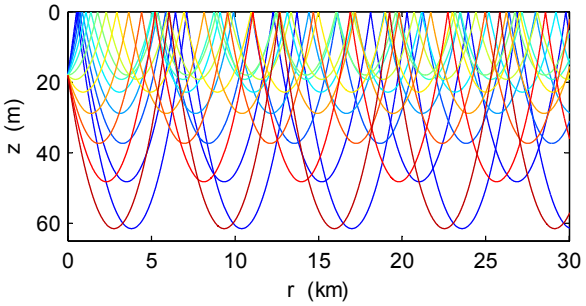


**Figure 9**. Ray plot for modelled scenario

**Table 2**. Spread of incidence angles at surface for modelled scenario, various wind speeds

| no wind | 5 m/s | 7.5 m/s | 10 m/s |
|---|---|---|---|
| surface sound speed 1500 m/s | surface sound speed 1498 m/s | surface sound speed 1493.5 m/s | surface sound speed 1484.5 m/s |
| 1.13°-2.16° | 3.04°-3.65° | 5.33°-5.87° | 8.01°-8.40° |

The increases in incidence angle may be determined from Snell's law. For example, if Snell's law is expressed as

$$\theta_1 = \arccos\left(\cos\theta_2 [c_1/c_2]\right) \text{ radians}, \qquad (5)$$

it may be applied to the limiting ray in the surface duct. Thus the sound speed ($c_2 = 1501.09$ m/s) corresponding to the turning point ($\theta_2 = 0.0°$) for the limiting ray at the bottom of the duct may be related, using (5), to the grazing angle $\theta_1$ at the surface, for which the sound speed is $c_1$.

For small angles expression (5) may be approximated to

$$\theta_1 \approx \sqrt{2c_\Delta/1500} \text{ radians,} \quad (6)$$

where $c_\Delta$ m/s is the difference in sound speed between that at the bottom of the surface duct and at the surface. If most of the value of $c_\Delta$ is attributed to the effect of near-surface bubbles, it follows that a value of $c_\Delta$ may be estimated as the change in surface sound speed caused by the bubbles, and so values of surface incidence angle $\theta_1$ may be estimated. For practical purposes, for transmission in a surface duct which has wind-generated bubbles it may be seen that all rays in the duct interact with the surface at effectively the same angle $\theta_1$ given by (6), with this angle being dependent upon wind speed. This does seem to be the case for the data in Table 2. An outcome from this is that the loss value, per bounce, for each ray that propagates in the duct is, very nearly, the same for every ray in the duct, and is insensitive to the launch angle.

In a practical sense, this means that surface loss per bounce for a model of transmission may be described, approximately, using an algorithm which is a function only of wind speed and frequency (if rms surface height is used in the model, it is assumed that this is obtained from wind speed via (1)). For practical applications of modelling surface ducted transmission, it may be convenient if surface loss can be described without explicit modelling of bubble effects. This then requires a model for which loss is relatively insensitive to the grazing angle anticipated for a bubble-free ocean, but is appropriate to the wind speed and frequency. This surprising result leads to the realisation that the Beckmann-Spizzichino models, for which data is shown in Fig. 1, 2 and 3, *do* provide this insensitivity to grazing angle, although for practical use such a model would need the appropriate dependence on wind speed and frequency.

For the modelled scenario, values of surface loss for use with a bubble-free model of the ocean may be obtained as follows: by taking the surface grazing angle obtained by (6), and then finding the corresponding loss value per bounce from the Williams et al. small slope model from the appropriate one of Fig. 1, 2 or 3, a suitable loss value per bounce may be found for all transmitting rays. These loss values are about 0.3 dB per bounce (5 m/s wind speed), 2.3 dB per bounce (7.5 m/s wind speed) and a value in excess of 10 dB per bounce (10 m/s wind speed). It may be noted from Figs. 1, 2 and 3, that neither of the two Beckmann-Spizzichino models produces a particularly good fit to all these loss values.

### Calculations of Transmission Loss

Calculation of *TL* were carried out for the test scenario for (i) bubble-free water with smooth ocean surface, (ii) loss due to surface roughness alone (described using the Williams et al. small slope model) and (iii) loss due to surface roughness and the refractive effects of a bubbly SSP. The *TL* was modelled using the BELLHOP model [18] as implemented via the CMST [19]. For modelling the coherent *TL*, a beam spacing of 0.00125° was used.

The data in Fig. 10 show that for wind speeds of 7.5 m/s and 10 m/s there is a substantial increase in the *TL* when the surface loss is modelled by the combination of the Williams et al. small slope model and the refractive effects of the wind-induced bubbles. This is consistent with the expectation of the previous section for surface loss values of 2.3 dB per bounce (7.5 m/s wind speed) and in excess of 10 dB per bounce (10 m/s wind speed). There is also an increase in *TL* for the case of wind speed 5 m/s, when the rough surface model is combined with the refractive effects of bubbles, however the increase is modest, being less than 5 dB at 30 km. Clearly, it is important that the bubble effects are included, otherwise the loss values are under-estimated.

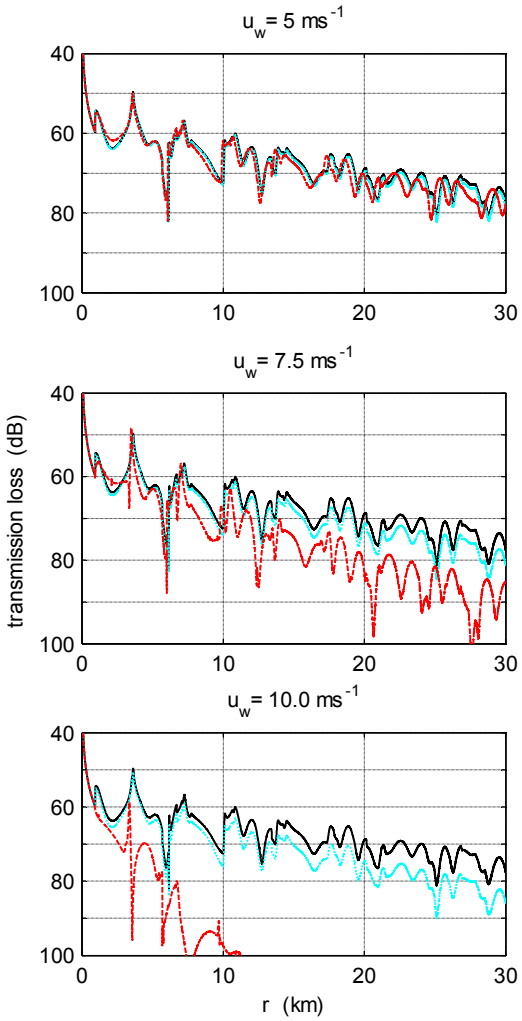


**Figure 10**. Transmission Loss for surface duct scenario: black – no surface loss; blue - Williams et al. roughness model [5]; red - Williams et al. roughness model [5] plus refraction caused by wind induced bubbles [12]

## CONCLUSIONS

A study was made of some of the practical aspects of modelling acoustic surface loss at small angles of incidence typical of surface ducted transmission within a real ocean. Most models of surface loss are, in fact, models of surface roughness loss, and do not explicitly include either the refractive or the scattering effects of wind induced bubbles which exist in the near-surface region. The Williams et al. small slope model of surface roughness loss [5], and its relationship to the Kirchhoff model, were examined. It was postulated that a rationale based on surface radius limits might be devised to predict a lower limiting grazing angle below which the Kirchhoff model fails and a simple correction might be made which would result in a reasonable approximation of the

more accurate Williams et al. result. The veracity of the Williams et al. small slope model was confirmed by deterministic modelling of the surface loss per bounce, using PE transmission modelling combined with random replications of a surface matching the Pierson-Moskowitz wave spectrum.

By including the refractive effects of near-surface wind-induced bubbles (after Ainslie [12]) with the Williams et al. small slope surface loss, increased transmission loss values were obtained in simulations of surface ducted transmission. The surprising result from inclusion of the bubble effects was, however, that the surface loss values per bounce could be shown to be wind speed dependent, but not dependent on the angle at which grazing incidence at the surface would be expected if bubbles were ignored. This then leads to the expectation that a practical model of surface loss, which provides the true loss value for a bubbly ocean, but is applied without the refractive effects of bubbles being explicitly described, would have a similar lack of grazing angle dependence as the Beckmann-Spizzichino-type models. These had been shown by the authors [9-11] to be wanting from the viewpoint of roughness losses alone. It then does appear that, for some ranges of wind speed values, a Beckmann-Spizzichino-type model similar to that used by RAYMODE [7, 8] may be "right, but for the wrong reason".

It now appears that the way ahead in surface loss modelling will require combining the effects of a model of surface roughness with the refractive effects of seawater with bubbles. A clear conclusion of this present work is that the effects on acoustic loss caused by wind-induced near surface bubbles are profound.

## REFERENCES


1 H.W. Marsh, M. Schulkin and S.G. Kneale, "Scattering of Underwater Sound by the Sea Surface", *J. Acoust. Soc. Am.*, **33**, 334 – 340 (1961)

2 H.W. Marsh and M. Schulkin, *Underwater Sound Transmission*, AVCO Marine Electronics Office, DTIC Accession Number AD294962 (1962)

3 H. Medwin, *Ocean Surface Reflection Loss: Status Report and Prediction Procedures*, Meteorology International Inc., Monterey, CA, ADA061984 (1968)

4 E.Y.T. Kuo, "Sea Surface Scattering and Propagation Loss: Review, Update and New Predictions", *IEEE J. Oceanic Eng.*, **13**, 229 – 234 (1988)

5 K.L. Williams, E.I. Thorsos and W.T. Elam, "Examination of coherent surface reflection coefficient (CSRC) approximations in shallow water propagation", *J. Acoust. Soc. Am.*, **116** (4), 1975 – 1984 (2004)

6 P. Beckmann and A. Spizzichino, *The Scattering of Electromagnetic waves from Rough Surfaces*, (Pergamon Press, 1963)

7 R.B. Lauer, *The Acoustic Model Evaluation Committee (AMEC) Reports, Volume III, Evaluation of the RAYMODE X Propagation Loss Model*, NORDA Report 36, Book 1 of 3, NORDA, NSTL Station, Mississippi, DTIC Accession Number ADC034021 (1982)

8 R.W. McGirr, *An analysis of surface-duct propagation loss modeling in SHARPS*, NORDA Report 209, Stennis Space Center, DTIC Accession Number AD-A239802 (1990)

9 A.D. Jones, J. Sendt, A.J. Duncan, Z.Y. Zhang and P.A Clarke, "Modelling acoustic reflection loss at the ocean surface – an Australian study", *Proceedings of ACOUSTICS 2008*, Geelong, Australia (2008)

10 A.D. Jones, J.Sendt, A.J. Duncan, P.A. Clarke and A.Maggi, "Modelling the acoustic reflection loss at the rough ocean surface", *Proceedings of ACOUSTICS 2009*, Adelaide, Australia (2009)

11 A.D. Jones, A.J. Duncan, A. Maggi, J. Sendt and P.A. Clarke, "Modelling acoustic reflection loss at the ocean surface for small angles of incidence", *Proceedings of IEEE OCEANS'10*, Sydney, Australia (2010)

12 M.A. Ainslie, "Effect of wind-generated bubbles on fixed range acoustic attenuation in shallow water at 1 – 4 kHz", *J. Acoust. Soc. Am.*, **118**, 3513 – 3523 (2005)

13 J.A. Ogilvy, "Wave scattering from rough surfaces", *Rep. Prog. Phys.* **50**, 1553-1608 (1987)

14 X. Lurton, *An Introduction to Underwater Acoustics,* (Praxis Publishing Ltd., Chichester, 2002), pp 314-315

15 L.M. Brekhovskikh and Yu.P. Lysanov, *Fundamentals of Acoustics*, 3rd edition (Springer-Verlag, New York, 2003)

16 R.J. Wagner, "Shadowing of Randomly Rough Surfaces", *J. Acoust. Soc. Am.*, **41** (1), 138 – 147 (1967)

17 H. Medwin and C.S. Clay, *Fundamentals of Acoustical Oceanography* (Academic Press, 1998)

18 http://oalib.hlsresearch.com

19 A.J. Duncan and A.L. Maggi, "A Consistent, User Friendly Interface for Running a Variety of Underwater Acoustic Propagation Codes", *Proceedings of ACOUSTICS 2006*, Christchurch, New Zealand, 471–477 (2006)

20 P.C. Etter, *Underwater Acoustic Modeling and Simulation*, 3rd edition, (Spon Press 2003)

21 G.B. Thomas, Jr., *Calculus and Analytic Geometry* (Addison-Wesley, Reading, Massachusetts, 1965), pp 585–590